ICEE 2020 1570693504

Design and Simulation of Capacitive Z-axis MEMS Accelerometers using SU-8, PolySi, Si3N4, and SiC-based structural materials

Mandeep Jangra
School of Computing and Electrical Engineering
IIT-Mandi
India
j.mandeep.hsr@gmail.com

Dhairya Singh Arya
School of Computing and Electrical Engineering
IIT-Mandi
India
dhairya_arya@yahoo.in

Robin Khosla
School of Computing and Electrical Engineering
IIT-Mandi
India
robinkhosla99@gmail.com

Satinder Kumar sharma
School of Computing and Electrical Engineering
IIT-Mandi
India
satinder@iitmandi.ac.in

***Abstract*— A comparative study of MEMS-based micro accelerometers with four different spring mechanism and four structural materials are presented in this paper. The serpentine spring design is used for the highly sensitive topographic structure after investigating various spring topography due to its reduced spring constant. The highly sensitive serpentine structure-based spring design is simulated for MEMS accelerometers with SU-8, PolySi, Si_3N_4, and SiC as primary structural materials. After UV exposure, the stiffness of the SU-8 polymer is considered to be varied and measured with the Nano-indentation technique, and the spring constant is calculated with the graphical method. Comparative study of different materials is shown by simulation using COMSOL Multiphysics 5.5. SU-8 being a polymer-based MEMS accelerometer with an acceleration sensitivity of ~357nm/g, shows high sensitivity and cost-effectiveness, suitable for industry compared to other conventional materials. SU-8 MEMS can be integrated with Si-technology for CMOS-based post-processing circuitry. The stress analysis investigates the spring and structural reliability of the designed micro accelerometers. The computational results of designed accelerometers showed a linear response up to ±50 g of acceleration's input value. The design of SU-8 highly sensitive, serpentine spring, low-cost and simplistic process technology-based Z-axis accelerometer shows the resonant frequency of 1.4 kHz, which is suitable for tactual, and navigation applications.**

Keywords— Microaccelerometer, Polymer MEMS, Capacitive MEMS Accelerometer, SU-8 MEMS

I. INTRODUCTION

Microelectromechanical systems (MEMS) accelerometers are widely used in consumer robotics, automotive, military, biomedical, and space applications [1-2]. Capacitive MEMS accelerometers out of different sensing schemes have attracted immense attention because of their high resolution, temperature, long-term stability, and simple fabrication process technology. These Accelerometers measure the change between a fixed electrode and a movable electrode on suspended proof mass [3]. An ideal accelerometer should havehigh sensitivity, large bandwidth (high working range of application), and low cost [4]. Numerous MEMS accelerometers are investigated in the literature. The main limitation of these MEMS accelerometers is the high cost and complicated process of costly fabrication. Therefore, other design structures having some acceptable performance parameters are worthy of investigation. The optimum performance of a MEMS accelerometer extensively depends on the structural material of the accelerometer. The majority of the commercial inertial sensors are fabricated using silicon as a preferable substrate because of its fabrication possibility at a higher temperature, high young's modulus, and lower thermal expansion. However, the fabrication of such sensors on the silicon substrate is complicated, involving complicated steps like deep reactive ion etching (DRIE), wet etching in KOH or TMAH, diffusion or ion implantation very costly as well as ends in higher residual stress. The proposed research work is expected to enhance the sensitivity, reduce cost, and fabrication process complexity.

There is a requirement for a simple, cost-effective accelerometer sensor in many daily life applications, fabricated with ease using the standard process at low manufacturing cost [5]. These demands have motivated the manufacturer to find a suitable material satisfying the above conditions. Recently, polymer-based MEMS accelerometers have gained significant attention from the scientific community. In past years, SU-8 has emerged as an alternative structural material, an active photo material. SU-8 is available in different thicknesses varying from 0.5µm to 200µm [6] with nomenclature SU-8 2000.5, 2002, 2025, 2100. This material's hardness can be controlled using photo exposure dose and baking temperature for the desired stiffness property. Due to being photosensitive, the SU-8 polymer's entire structure/patterns, especially proof mass, supporting springs, and MEMS accelerometer anchors, can be fabricated using lithography techniques at room temperature only [7-11]. In this work, we have compared four different spring topologies and four different conventional structural materials. Analyzing the best combination of spring topology and structural material, we have used SU-8 as a structural material to design the entire device on a dummy silicon substrate with no active participation of silicon with serpentine spring topology.

978-1-7281-8660-3/20/$31.00 @2020 IEEE

2020 5th IEEE International Conference on Emerging Electronics (ICEE) | 978-1-7281-8660-3/20/$31.00 ©2020 IEEE | DOI: 10.1109/ICEE50728.2020.9776817

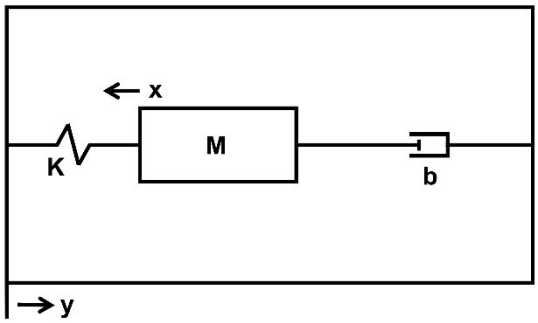

Fig. 1 Spring Mass Damper System

Because of the low young modulus of SU-8, i.e., ~4 GPa microstructure, it has relatively higher deflection sensitivity than silicon, and because of such properties, SU-8 has been used in many MEMS applications [12]. Based on process parameters, different thicknesses of microstructure can be fabricated using SU-8 photoresist material. Durable interlayer adhesion, good thermal permanency, and high performance to cost ratio are other reasons for picking this material for structural material for the MEMS accelerometer [5,13].

In this paper, a comparison of SU-8 material has been shown with other conventional materials along with different characteristics analysis using FEM Simulations.

II. Principle of Operation

An Accelerometer is modeled as a spring-mass damper system shown in fig. 1, in which deflection is produced in proof mass with the acceleration of the system. This deflection is recorded as an electrical signal. Equation (1) explains the Spring mass damper system.

$$F = -kx - b\dot{x} \tag{1}$$

where F is the force experienced by mass (m), k is spring. Constant, and b is the damping coefficient. If we further solve this equation for the spring-mass damper system, then we get equation (2) given below

$$\frac{x}{a} = \frac{-1}{s^2+2\xi\omega_o s+\omega_o^2} \tag{2}$$

where $\omega_o = \sqrt{k/m}$ and $\xi = b/2\ \omega_o m$ is called the resonant frequency and the damping ratio, respectively. Since ω_o is the function of m and k. So, on increasing the value of k, ω_o will increase, but at the same time, the sensitivity will decrease.

III. Design and Simulation

FEM Analysis:

All simulation results are carried out using COMSOL Multiphysics 5.5. Solid mechanics and MEMS modules are used for Simulation and performance analysis. Device designs and structures used for FEM analysis are shown in fig. 2. Proof mass dimensions (LxWxH) are 1500x1500x20 (µm x µm x µm) with 100nm top electrode layer of aluminium. Bottom layer of the same thickness is below proof mass on the substrate. The gap between the proof mass and bottom electrode is kept 80 µm Designed structures and structural materials are explained in the subsection.

A. Spring topologies

The sensitivity of the accelerometer and spring constant has an inverse relationship. For the optimization purpose, different spring topologies are investigated and computed using a force-deflection slope (Fig. 3). Initially, other

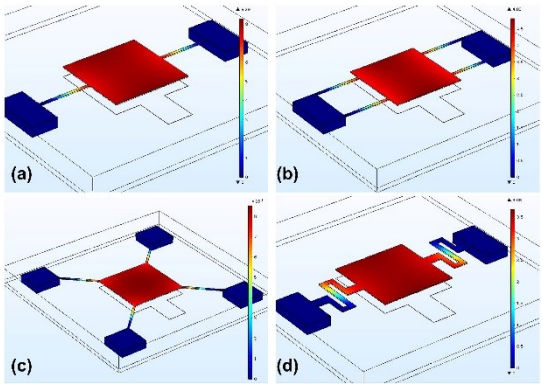

Fig. 2 The structure of spring topologies (a) Single beam, (b) Double beam in parallel, (c) Double beam in the corner, and (d) Serpentine.

prototype spring structures with the proof mass in the center are designed and simulated such as (i) Single-beam (Fig. 2(a)), (ii) Double beam in parallel (Fig. 2(b)), (iii) Double beam in the corner (Fig. 2(c)), and (iv) Serpentine (Fig. 2(d)). The calculated spring constant for single beam, double beam in parallel, double beam in the corner, and serpentine spring structures is ~11.3, ~19.2, ~33.5, and ~8.42

respectively. Deflection sensitivity at an acceleration of 50g

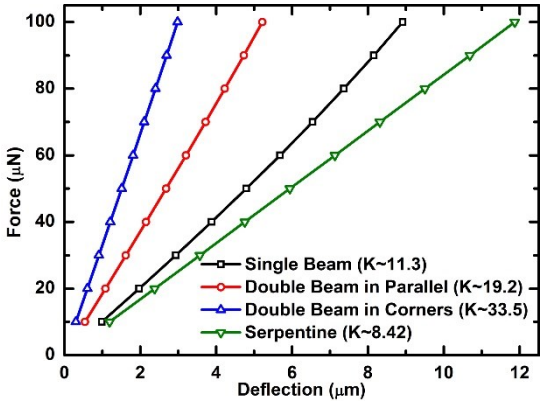

Fig. 3 Force-Deflection Characteristics for various spring topologies simulated for (i) Single beam, (ii) Double beam in parallel, (iii) Double beam in corner, and (iv) Serpentine.

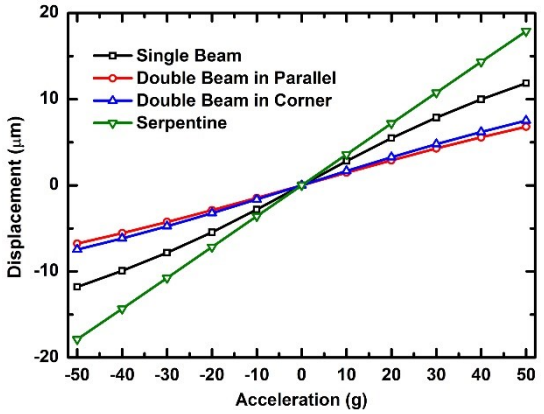

Fig. 4 Relationship between movable mass displacement and acceleration for, (i) Single beam, (ii) Double beam in parallel, (iii) Double beam in corner, and (iv) Serpentine spring topologies.

for single beam, double beam in parallel, double beam in corner, and serpentine spring structures is ~11.85 µm, ~6.80 µm, ~7.51 µm, and ~17.88 µm, respectively, which are represented graphically in fig.4. Thus, it confirms that serpentine spring has the highest sensitivity among all designs investigated here. The spring constant and displacement sensitivity of all spring designs are summarized in table 1.

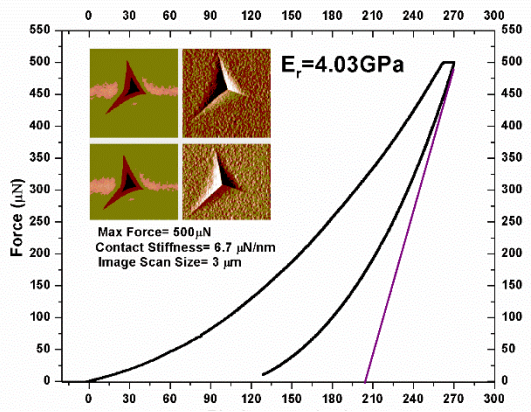

Fig. 5 The Force-Displacement (P-h) for the calculation of young's modulus of SU-8 material after UV exposure. The inset displays the Berkovich diamond indenter tip which is used for nanoindentation. Copyright 2021 Springer Nature [19]

Serpentine spring's performance is more agreeable to comply than other springs of fixed straight beams of the same length. Technically, serpentine spring has 4-5 beams connected in series having spring constant k for each beam, then the inverse of total spring constant of serpentine spring becomes equals to the sum of the inverse of spring constant of each beam connected in series giving a reduced value of spring constant for entire structure [14]. Serpentine spring design having better sensitivity among all are considered for further simulation of different structural materials. The serpentine spring design, shown in fig. 2(d), is used for simulation and comparison with other structural materials.

Table 1. Comparison of different spring topologies

Parameter	Spring Design			
	serpentine	Double beams in corners	Double beams in parallel	Single beam
Spring constant	8.42	33.5	19.2	11.3
Displacement (um) at 50g acceleration	17.88	7.51	6.80	11.85

B. Structural materials

Four different materials (SU-8, Poly-Si, Si_3N_4, and SiC) have been used to simulate the serpentine spring design accelerometer. Material parameters are given in table 2. Here, the young modulus of SU-8 is estimated by the Nanoindentation technique. Material characterization results from nano-indentation techniques are shown in fig. 5. Table 2 lists the mechanical properties of materials used for simulations. Proof mass of the SU-8, Poly-Si, Si_3N_4, and SiC are ~54 x 10^{-9}, ~104 x 10^{-9}, ~140 x 10^{-9}, and ~144 x 10^{-9} Kg, respectively. Further, the displacement and acceleration behavior of accelerometers having different structural materials are analyzed with simulation up to ±50g. Fig. 6 shows the displacement of proof mass up to 50 g with different structural materials. It is clear that SU-8 based device has the highest displacement sensitivity as 357.7nm/g. In contrast, other materials have shown displacement sensitivity as ~12.50, ~11.33, ~4.18 nm/g for Poly-Si, Si_3N_4, and SiC structural materials-based accelerometers with serpentine spring structure, respectively. Fig. 7 depicts serpentine spring-based accelerometers' frequency response with SU-8, Poly-Si, Si_3N_4, and SiC as structural materials. The simulated resonance frequency of SU-8, Poly-Si, Si_3N_4, and SiC structural materials-based accelerometers is estimated to be ~1.39, ~4.21, ~4.80, and ~9.10 kHz, respectively. The reasonable resonant frequency of the SU-8 structural material-based accelerometer is due to

Table 2. Material properties of the materials used for simulation [15-17]

Parameters	Materials			
	SU-8	Poly-Si	Si_3N_4	SiC
Density (kg/m^3)	1200	2320	3100	3216
Young's modulus (GPa)	4.03	169	250	748
Poisson Ratio	0.22	0.22	0.23	0.45

the high displacement of SU-8, which leads to lower resonant frequency (f_r) as per equation (3) and reveals its potential for navigation, space, and medical applications, etc..

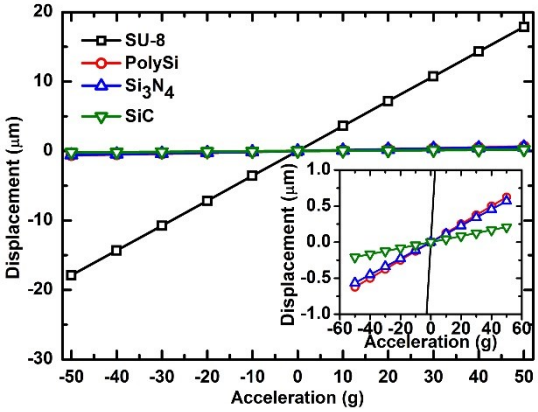

Fig. 6. Simulation results showing relationship between movable mass displacement and acceleration for SU-8, Poly-Si, Si_3N_4, and SiC structural material based accelerometers with serpentine spring structure.

$$f_r = \frac{1}{2\pi}\sqrt{\frac{F}{mx}} \tag{3}$$

Further, stress analysis is also performed and simulated to check the reliability of the spring structure. In the simulation, we checked von misses stress, which is a popular stress analysis method. In constant applied acceleration vs. generated stress on SU-8, Poly-Si, Si_3N_4, and SiC material-based devices are plotted in fig. 8. The generated stress should

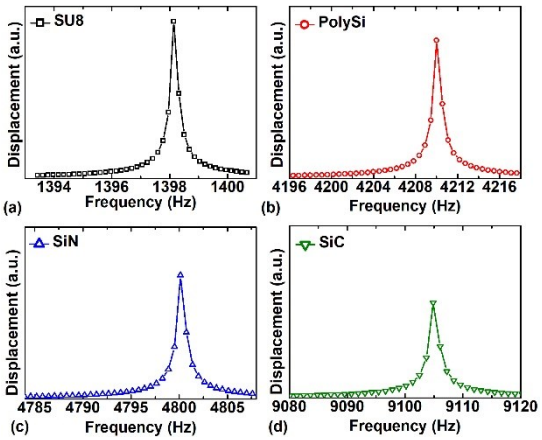

Fig. 7 Simulation results showing frequency Response of serpentine spring based MEMS accelerometers with SU-8 (a), Poly-Si (b), Si_3N_4 (c) and SiC (d) as structural materials.

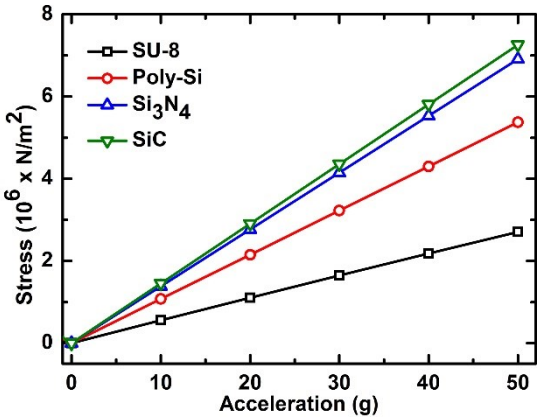

Fig. 8 Simulation results showing stress analysis of SU-8, Poly-Si, Si_3N_4 and SiC structural materials based accelerometers with serpentine spring structure.

be less than the material's yield point for the device's survival and reliability. The generated stress for SU-8, Poly-Si, Si_3N_4, and SiC structure materials based accelerometers at 50g of input acceleration is estimated to be ~2.7 x 10^6, ~5.4 x 10^6, ~6.9 x 10^6, and ~7.2 x 10^6 N/m^2, respectively for the serpentine based design which is much lesser than the yield point of ~0.06 x 10^9 N/m^2 in the case of SU-8 and ~7-14 x 10^9 N/m^2 in case of PolySi, SiC, and Si_3N_4 [18]. Simulated structural materials are reliable and survivable in a given limit of acceleration. The required performance parameters of MEMS accelerometer-based on SU-8, Poly-Si, Si_3N_4, and SiC are summarized in table 3. Simulated results show that SU-8 has future scope for the fabrication of MEMS accelerometers with high displacement sensitivity.

Table 3 Comparison of different structural Materials

Parameters	Materials			
	SU-8	Poly-Si	Si_3N_4	SiC
Displacement sensitivity (nm/g)	357.68	12.50	11.33	4.18
Resonant Frequency (kHz)	1.39	4.21	4.80	9.10
Stress @ 50g (10^6 N/m^2)	2.7	5.4	6.9	7.2

IV. Conclusion

Serpentine spring structure has shown the highest sensitivity among remaining single beam, double beam in parallel, and double beam in the corner architecture. Four different materials (SU-8, polysilicon, silicon nitride, and silicon carbide) are used to simulate the MEMS accelerometer with serpentine spring architecture. SU-8 being a polymer-based MEMS accelerometer with an acceleration sensitivity of ~357 nm/g shows high sensitivity than other conventional materials. The stress analysis investigates the spring and structural reliability of the designed micro accelerometers that offer the accelerometer's survivability. The computational results of designed accelerometers showed a linear response up to ±50 g of acceleration's input value. The design of SU-8 based highly sensitive, serpentine spring, low-cost and simplistic process technology-based Z-axis accelerometer shows a resonant frequency of ~1.4 kHz. Finally, the fabrication and characterization of SU-8 based micro accelerometers have scope for future work.

Acknowledgment

The authors acknowledge the financial support of seed grant project IIT/SG/SKS/27, Indian Institute of Technology (IIT), Mandi, Himachal Pradesh, India.

References

[1] N. Yazdi, F. Ayazi, and K. Najafi "Micromachined inertial sensors" Proc. IEEE vol. 86, pp. 1640, 1998.

[2] A. Alvin Barlian, Woo-Tae Park, Joseph R. Mallon, Jr., Ali J. Rastegar, and Beth L. Pruitt "Review: semiconductor piezoresistance for Microsystems" Proc. IEEE Vol. 97, pp. 513, 2009.

[3] V. Kumar, R. Jafari, and S. Pourkamali, "Ultra-Low Power Digitally Operated Tunable MEMS Accelerometer", IEEE Sensors Journal, vol. 16, no. 24, pp. 8715, 2016.

[4] S. J.-Michel, "Market opportunities for advanced MEMS accelerometers and overview of actual capabilities vs. required specifications", PLANS 2004, Position Location and Navigation Symposium , Monterey, CA, USA, pp. 78, 2004.

[5] V. Seena, K. Hari, S. Prajakta, R. Pratap, and V. R. Rao, "A novel piezoresistive polymer nanocomposite MEMS accelerometer," J. Micromech. Microeng. vol. 27, pp. 015014, 2017.

[7] R. Patkar, P. Apte,&V. Rao, A novel SU8 polymer anchored low temperature HWCVD nitride polysilicon piezoresitive cantilever. Journal of Microelectromechanical Systems, 23(6),pp. 1359-1365. 2014.

[8] R. Rahimi, M. Ochoa,W. Yu,and B. Ziaie, Highly stretchable and sensitive unidirectional strain sensor via laser carbonization. ACS applied materials & interfaces, 7(8), pp.4463-4470, 2015.

[9] M. Soni, T. Arora, R. Khosla, P. Kumar, A. Soni and S. K. Sharma, "Integration of Highly Sensitive Oxygenated Graphene With Aluminum Micro-Interdigitated Electrode Array Based Molecular Sensor for Detection of Aqueous Fluoride Anions," IEEE Sensors Journal, vol. 16, no. 6, pp. 1524, 2016.

[10] S. Sharma, S. Das, R. Khosla, H. Shrimali and S. K. Sharma, " Realization and performance analysis of facile-processed µ-IDE-based multilayer HfS_2/HfO_2 transistors", IEEE Trans. Electron Devices, vol. 66, no. 7, pp. 3236-3241, Jul. 2019.

[11] T.R. Michel, M.J. Capasso, M.E. Cavusoglu, J. Decker, D. Zeppilli, C. Zhu, S. Bakrania, J.A. Kadlowec, and W. Xue, Evaluation of porous polydimethylsiloxane/carbon nanotubes (PDMS/CNTs) nanocomposites as piezoresistive sensor materials. Microsystem Technologies, 26(4), pp.1101-1112, 2020.

[12] V. Seena, A. Fernandes,P. Pant, S. Mukherji, and V.R. Rao, Polymer nanocomposite nanomechanical cantilever sensors: material characterization, device development and application in explosive vapour detection. Nanotechnology, 22(29), pp.295501, 2011

[13] L. Gammelgaard, P.A. Rasmussen, M. Calleja, P. Vettiger, and A. Boisen, Microfabricated photoplastic cantilever with integrated photoplastic/carbon based piezoresistive strain sensor. Applied Physics Letters, 88(11), pp.113508, 2006

[14] M.-H. Bao, Micro mechanical transducers: pressure sensors, accelerometers, and gyroscopes, vol. 8. 2000

[15] T. Yi and C. Kim, "Measurement of mechanical properties for MEMS materials", Measurement Science and Technology vol. 10, no. 8, 1999.

[16] H. Search, C. Journals, A. Contact, M. Iopscience, and I. P. Address, "Elastic properties and microstructure of LPCVD polysilicon films," J. Micromech. Microeng., vol. 6. no. 4, 1996.

[17] H. Search, C. Journals, A. Contact, and M. Iopscience, "Structure, mechanical properties, and thermal transport in microporous silicon nitride - molecular-dynamics simulations," EPL (Europhysics Letters) vol. 33, no. 9, 1996

[18] M. Madou, "Principal source for semiconductor material properties: "Fundamentals of Microfabrication", CRC Press, 1997.

[19] M, Jangra, D S Arya, R Khosla, and S K. Sharma. "Maskless lithography: an approach to SU-8 based sensitive and high-g Z-axis polymer MEMS accelerometer." Microsystem Technologies pp 1-10, 2021.